



Labrador current variability over the last 2000 years



M.-A. Sicre^{a,b,*}, K. Weckström^c, M.-S. Seidenkrantz^d, A. Kuijpers^c, M. Benetti^b,
G. Masse^e, U. Ezat^b, S. Schmidt^f, I. Bouloubassi^a, J. Olsen^g, M. Khodri^a, J. Mignot^{a,h}

^a Laboratoire d'Océanographie et du Climat: Expérimentation et Approches Numériques (LOCEAN), IPSL-UPMC/CNRS/IRD/MNHN, Paris, France

^b Laboratoire des Sciences du Climat et de l'Environnement, IPSL/CNRS/CEA, Gif-sur-Yvette Cedex, France

^c Geological Survey of Denmark and Greenland, Department of Marine Geology and Glaciology, Copenhagen, Denmark

^d Centre for Past Climate Studies and Arctic Research Centre, Department of Geoscience, Aarhus University, Denmark

^e Takuvik, UMI 3376, 1045 Avenue de la Médecine, G1V 0A6 Québec, QC, Canada

^f CNRS EPOC, UMR 5805, F-33400, Université Bordeaux-1, Talence, France

^g The Aarhus AMS ¹⁴C Dating Centre, Department of Physics and Astronomy, Aarhus University, Denmark

^h Climate and Environmental Physics, Physics Institute, University of Bern, Switzerland

ARTICLE INFO

Article history:

Received 12 September 2013

Received in revised form 15 April 2014

Accepted 7 May 2014

Available online 2 June 2014

Editor: J. Lynch-Stieglitz

Keywords:

ocean variability

temperature proxy

last millennia

Labrador Sea

Newfoundland

Northern Annular Mode

ABSTRACT

The ice-loaded Labrador Current (LC) is an important component of the western North Atlantic circulation that influences the position and strength of the northern limb of the North Atlantic Current (NAC). This flow of cold and fresh Polar Waters originating from the Arctic has a marked impact on the North Atlantic climate, yet little is known about its variability beyond the instrumental period. In this study, we present the first sub-decadal alkenone-based 2000-year long sea-surface temperature (SST) records from the western Labrador Sea, a climatically crucial region at the boundary between the LC and the NAC. Our results show a clear link between the LC strength and the Northern Annular Mode (NAM), with a stronger NAM and a more vigorous LC during the Medieval Climate Anomaly (MCA). This suggests enhanced LC activity upon future global warming with implications for the Atlantic meridional overturning circulation (AMOC).

© 2014 Elsevier B.V. All rights reserved.

1. Introduction

Climate in the North Atlantic region is strongly influenced by Arctic Ocean waters exported to the mid-latitudes of the North Atlantic Ocean through Fram Strait (Eastern Route) and the Canadian Archipelago/western Labrador Sea (Western Route) (Fig. 1). These low-density waters affect deep convection in the Labrador and Greenland Seas and, subsequently, the strength of the global thermohaline circulation and climate (Jones and Anderson, 2008). The LC accounts for about two thirds of the freshwater outflow from the Arctic Ocean (Aksenov et al., 2010). A sharp front separates the fresh and cold shelf waters of this boundary current from the warmer and saltier open-ocean waters of the Labrador Sea. Before reaching Hamilton Bank (ca. 54° N) offshore Labrador, the LC splits into a major outer branch trapped at the edge of the continental slope, and a minor inner branch (~15% of the total transport) flowing over the Newfoundland shelf (Lazier and Wright, 1993). Along its path, the LC has little exchange with the central Labrador

Sea. In the region of Flemish Cape and the Grand Banks east of Newfoundland, the LC retroflects northwards when encountering the North Atlantic Current (NAC) (Fratantoni and McCartney, 2010). The resulting freshening and cooling of the NAC on its way to the Nordic Seas are crucial processes controlling the rate and intensity of the AMOC, thus impacting European climate (Czaja and Frankignoul, 2002).

Today, the LC variability and the position of the northern edge of the NAC are strongly influenced by the Northern Annular Mode (NAM) (Dickson et al., 1996), which is defined from sea level atmospheric pressure between 20° and 90° N and reflects the degree of penetration of Arctic air into mid-latitudes. Deep Ice-landic lows during +NAM years favor NW winds bringing cold air from the Arctic over the Labrador Sea, which results in colder-than-normal winter SSTs, sea-ice formation and enhanced transport of ice-loaded LC waters (Drinkwater, 1996). In contrast, weaker Westerlies and more frequent southerly winds during -NAM years reduce winter ocean heat loss and promote warmer SSTs. NAM also induces changes in the Arctic Water gateways with implications for the deep convection. Under -NAM conditions, the Transpolar Drift of Polar Waters shifts eastwards towards Fram

* Corresponding author. Tel.: +33 1 44 27 84 14; fax: +33 1 44 27 49 93.

E-mail address: Marie-Alexandrine.Sicre@locean-ipsl.upmc.fr (M.-A. Sicre).

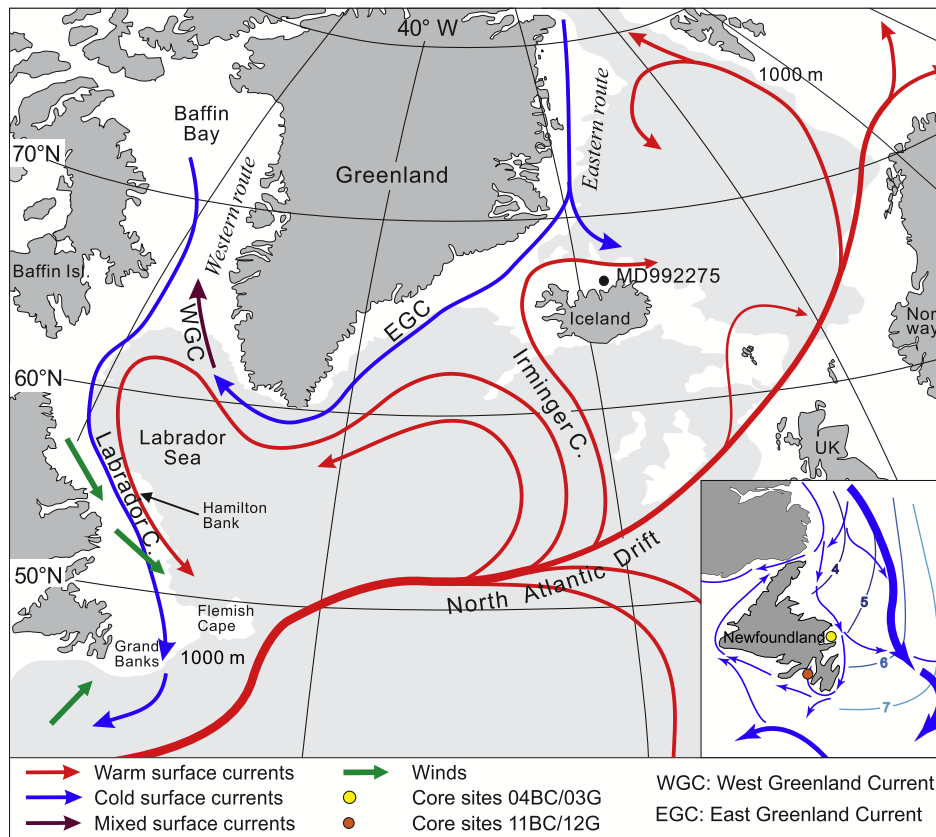


Fig. 1. Map showing North Atlantic surface currents, the study area, regional wind directions and the coring sites. Red/blue arrows indicate warm/cold surface currents, respectively; the prevailing wind directions are marked with light blue arrows. Core sites are shown on the insert map with the detailed surface hydrology of the Newfoundland area (thick blue arrows = Outer Labrador Current, thin blue arrows = Inner Labrador Current). Also shown in the insert are SST isolines (in °C) based on the NODC (Levitus) World Ocean Atlas 1998 (1.0 degree latitude \times 1.0 degree longitude global grid; 10 meter depth; data provided by the NOAA/OAR/ESRL PSD, Boulder, Colorado, USA, from their Web site at <http://www.esrl.noaa.gov/psd/>). The isolines represent April–June means for the years 1900–1997, thus largely overlapping with the time period covered by our two box cores. (For interpretation of the references to color in this figure legend, the reader is referred to the web version of this article.)

Strait (Morison et al., 2012). The East Greenland Current (EGC)/West Greenland Current (WGC) system is subsequently enhanced, which intensifies buoyancy-driven transport (Dickson et al., 1996) and leads to a more southerly NAC, as seen during the persistent and extreme $-$ NAM phase in the late 1960s (the ‘Great Salinity Anomaly’ (GSA)) (Dickson et al., 1988). Buoyancy gain combined with diminished ocean heat loss reduces deep convection in the central Labrador Sea and thus weakens the subpolar gyre (SPG) circulation (Dickson et al., 1996). In contrast, under $+$ NAM conditions, Arctic Waters are routed through the Canadian Archipelago and the LC transport increases under the influence of stronger NW winds (Fratantoni and McCartney, 2010). Concurrently, increased ocean heat loss favors enhanced convection in the central Labrador Sea, thus reinforcing SPG circulation and mixing with subtropical waters through the intergyre circulation (Marshall et al., 2001).

In recent years, efforts have been made to produce high-resolution SST reconstructions of the last millennia (PAGES 2k Consortium, 2013; Cunningham et al., 2013). However, despite its significance for the AMOC, the Labrador Sea region has hitherto remained poorly documented at decadal time scales over the past thousand years. Here, we present two sub-decadal alkenone-derived SST records from northeastern and southeastern Newfoundland coastal waters covering the last 2000 years. The NE site was selected to be representative of LC waters, while the SE site is located in the boundary zone between the LC and the Gulf Stream. The alkenone records thus allow us not only to track changes in SSTs but also to evaluate variations of the LC/Gulf Stream boundary.

2. Material and methods

2.1. Sediment sampling

A set of one box-core and one gravity core were collected at each study site during the research cruise on the Russian RV *Akademik Ioffe*, September 23–28, 2007. Box-core AI07-04BC (39.5 cm) and gravity core AI07-03G (460 cm) were retrieved from Bonavista Bay (48°44 N, 53°29 W; 329 m depth), offshore northeastern Newfoundland (Fig. 1). Box-core AI07-11BC (47°14 N; 54°36 W, 233 m water depth, 41 cm) and gravity core AI07-12G (47°08 N; 54°33 W; 230 water depth, 459 cm) were collected in Placentia Bay, off southeastern Newfoundland. The cores were taken from small sedimentary basins identified by a Parasound sub-bottom profiler and show no evidence of sediment re-working. Strong currents prevail over the shelf, but local sedimentary basins in fjords and open bays in direct connection to the open ocean offer suitable sedimentary conditions. The box-cores were analyzed every 0.5 cm over the first 2 cm, and then every 1 cm. The gravity cores were analyzed every 0.5 cm.

2.2. Sediment dating

Dating of the box-cores (AI07-04BC and AI07-11BC) was performed from excess activity of ^{210}Pb ($^{210}\text{Pb}_{\text{xs}}$) (Weckström et al., 2013). ^{210}Pb , ^{226}Ra and ^{137}Cs activities were analyzed using a low background, high efficiency, well-shaped γ detector (Schmidt et al., 2009), calibrated with certified reference material (IAEA-RGU-1). Activities are expressed in mBq g^{-1} and errors

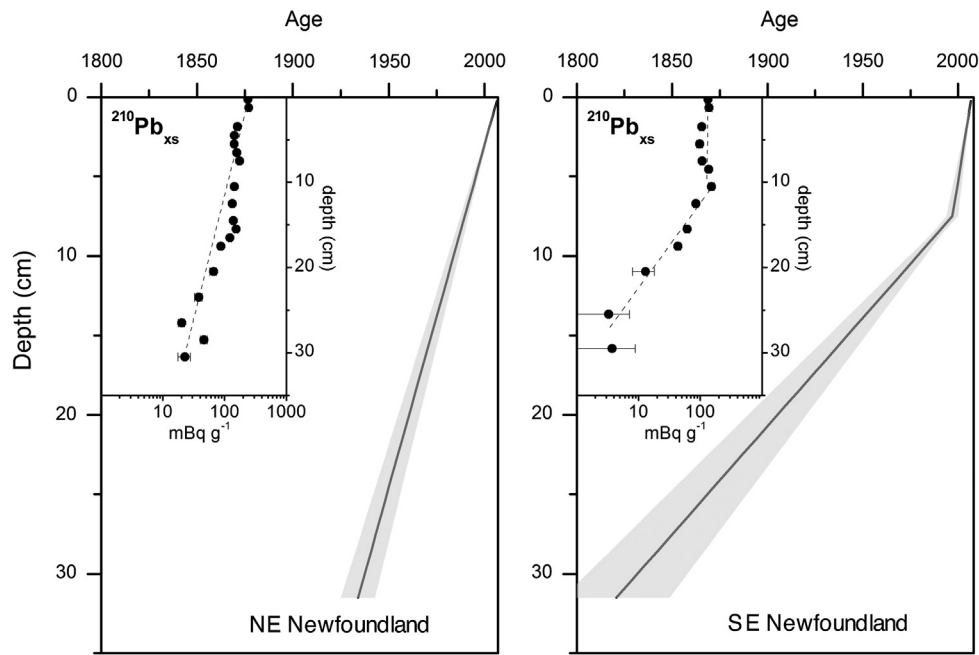


Fig. 2. ^{210}Pb profiles of box-cores AI07-04BC and AI07-11BC and age models established from the ^{210}Pb data.

Table 1

AMS ^{14}C dates and calibrated ages (in year AD) for the AI07-03 and AI07-12G gravity cores. Outliers were not included in the age model.

Core depth (cm)	Lab. code	Material	^{14}C age $\pm 1\sigma$ (yr BP)	ΔR	Calibrated age range, 95% confidence (cal. yr BP)	Modeled age (cal. yr BP)	$\delta^{13}\text{C}$ (‰VPDB)
<i>AI07-03G</i>							
35–37	AAR-12702	Mixed benthic foram.	1181 \pm 35	139 \pm 61	721–504	620 \pm 68	−2.97 \pm 0.05
44–45	AAR-16629	Shell	1481 \pm 24	139 \pm 61	1032–734	Outlier	44.5
60–61	AAR-12268	Mixed benthic foram.	1516 \pm 30	139 \pm 61	1075–755	910 \pm 80	−3.32 \pm 0.05
88–89	AAR-16630	Shell	1785 \pm 35	139 \pm 61	1334–1043	1204 \pm 85	5.5 \pm 0.8
110–111	AAR-16623	Shell	1940 \pm 26	139 \pm 61	1507–1233	1423 \pm 92	0.68
120.5–121.5	AAR-16624	Shell	2131 \pm 27	139 \pm 61	1715–1378	1566 \pm 96	0.64
151–152	AAR-12703	Mixed benthic foram.	2463 \pm 38	139 \pm 61	2131–1766	1979 \pm 107	0.51 \pm 0.05
<i>AI07-12G</i>							
30–32	AAR-12638	Mixed benthic foram.	1026 \pm 36	139 \pm 61	635–369	474 \pm 78	−0.96 \pm 0.05
55–57	AAR-16625	Shell	1143 \pm 30	139 \pm 61	683–489	630 \pm 72	0.64
100	AAR-16626	Shell	1872 \pm 35	139 \pm 61	1440–1129	Outlier	0.37
116–117	AAR-16627	Shell	1855 \pm 24	139 \pm 61	1400–1123	1290 \pm 84	0.05
131–132	AAR-16628	Shell	2163 \pm 26	139 \pm 61	1760–1410	Outlier	4.7 \pm 1
150–153	AAR-12639	Mixed benthic foram.	2235 \pm 70	139 \pm 61	1894–1440	1717 \pm 113	−1.03 \pm 0.05

are based on 1 SD counting statistics. Excess ^{210}Pb was calculated by subtracting the activity supported by its parent isotope, ^{226}Ra , from the total ^{210}Pb activity in the sediment. Errors in $^{210}\text{Pb}_{\text{xs}}$ were calculated by propagation of errors in the corresponding pair (^{210}Pb and ^{226}Ra). The sedimentation rate was calculated from $^{210}\text{Pb}_{\text{xs}}$ profiles using a constant flux-constant sedimentation (CF:CS) model. The SE Newfoundland core displays a two-layer $^{210}\text{Pb}_{\text{xs}}$ profile, which was taken into account when calculating the sedimentation rate. Age models were calculated assuming an age of 2007 at the core-tops. No clear signs of disturbance caused by bioturbation are observed in the surface sediments. Furthermore, the lithology of the gravity cores indicates fine laminations throughout the sediment sequence, which provides evidence for the sedimentary record being undisturbed by biological reworking.

The age models for the gravity cores (AI07-03G and AI07-12G) were established using the depositional model option in the OxCal 4.1 software using marine ^{14}C calibration curve Marine09 with an average ΔR of 139 \pm 61 years (Solignac et al., 2011; Jessen et al., 2011; Reimer et al., 2009) (Table 1). Core AI07-03G spans the last 5740 years (age of core-top 170 \pm 90 cal yr BP according to the age

model), with sedimentation rates ranging from 36 to 143 cm/kyr. Only the age model for the last 2000 years is shown here (Fig. 3). The age model is based on 7 AMS ^{14}C dated samples of mixed benthic foraminifera or shell fragments (1 outlier) and was constructed with a k -value of 150 yielding an agreement index of A_{model} of 110%. AI07-12G covers the last 6000 years, with the core-top at 176 \pm 102 cal. yr BP, and sedimentation rates ranging from 69 and 98 cm/kyr. The age model of the last 2000 years (Fig. 3) is based on 6 AMS ^{14}C dated mixed benthic foraminifera and shell fragments (2 outliers) and was constructed with a k -value of 50 yielding an agreement index of A_{model} of 84%. Age model uncertainties range from \sim 70–110 years (core AI07-03G) and \sim 70–115 years (core AI07-12G).

2.3. Alkenone analyses

Alkenones were extracted from freeze-dried sediments (methanol/methylene chloride; 1:2 v/v), purified by open column silica gel chromatography and then analyzed by gas chromatography on a Varian CX3400 equipped with a CP-Sil-5 capillary column (50 m \times 0.32 mm i.d.) and a flame ionization detector

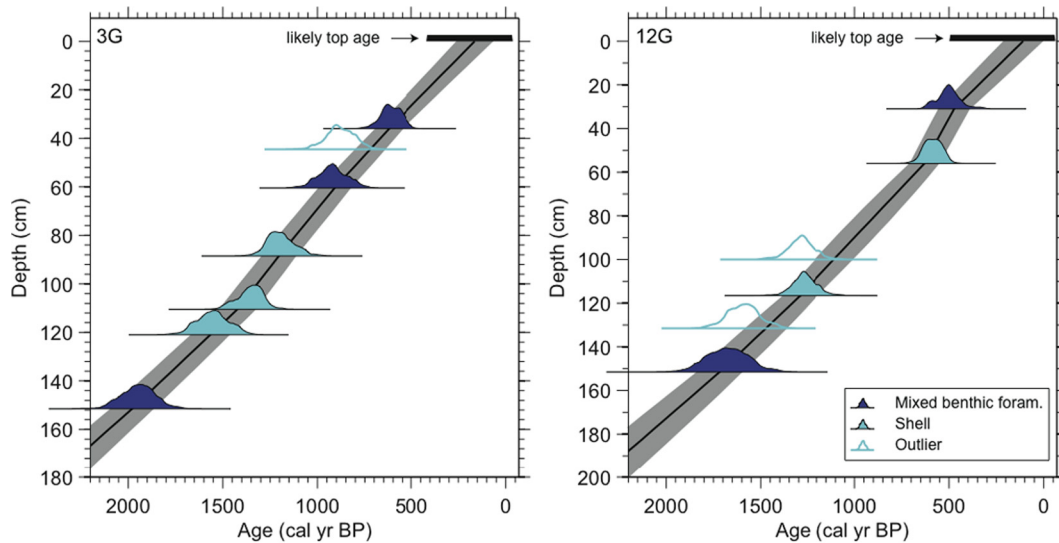


Fig. 3. Age model of gravity cores AI07-03G and AI07-12G based on calibrated ^{14}C dates. The age models were established with the depositional model option in the OxCal 4.1 software using marine ^{14}C calibration curve Marine09 with an average ΔR of 139 ± 61 years (Solignac et al., 2011; Reimer et al., 2009).

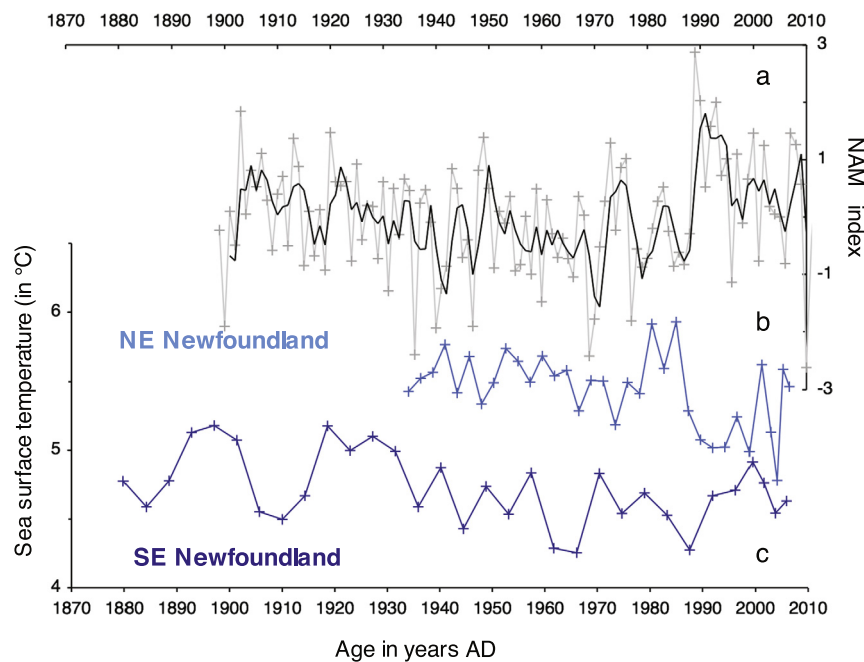


Fig. 4. Comparison of alkenone-derived SST reconstructions from recent sediments and NAM index values. (a) the NAM index was obtained from <http://climatedataguide.ucar.edu/guidance/hurrell-wintertime-slp-based-northern-annular-mode-nam-index>. The thick black line is the running 3-year mean, i.e. the temporal resolution of our proxy record (b) alkenone-derived SSTs off NE Newfoundland (Bonavista Bay; box-core AI07-04BC) in light blue, and (c) off SE Newfoundland (Placentia Bay; box-core AI07-11BC) in dark blue. (For interpretation of the references to color in this figure legend, the reader is referred to the web version of this article.)

(Terrois et al., 1996). SSTs were calculated from the U_{37}^K index $C_{37:2}/(C_{37:2} + C_{37:3})$ using the calibration of Prahl et al. (1988) ($SST = (U_{37}^K - 0.039)/0.034$). Internal precision for SST estimates is less than 0.5°C (Terrois et al., 1996).

3. Results and discussion

3.1. Alkenone-SST signal over the recent decades

SSTs for the recent decades were obtained from the two box-cores (AI07-04BC; AI07-11BC) (locations shown in Fig. 1) and compared to the NAM index (Fig. 4a). The NE Newfoundland record covers 80 yrs (AI07-04BC; 1925–2007 AD) while the SE Newfoundland one spans 125 yrs (AI07-11BC; 1880–2007 AD), the former allowing a higher temporal resolution (2.5 yrs) than the latter

(4.1 yrs) (Fig. 4b, c). SSTs vary between 4.5 and 5.5°C off NE Newfoundland, and between 3.5 and 4.5°C , off SE Newfoundland. This is at odds with the generally warmer instrumental SSTs in SE Newfoundland (Fig. 5), suggesting differences in the alkenone production patterns between the two sites.

Today, the NE Newfoundland site is mainly influenced by the LC and sea-ice covered for 2–3 months per year (± 1 month) (http://nsidc.org/data/docs/noaa/g00799_arctic_southern_sea_ice_index.html). SSTs range from 0.5°C in winter to $\sim 11^\circ\text{C}$ in summer (annual mean 4.2°C) (Fig. 5). Off SE Newfoundland SSTs are slightly higher, spanning from 0.9°C in winter to 12.5°C in summer (annual mean 5.4°C) (Fig. 5). This site, located at the southern edge of the LC where it borders towards the NAC, is generally ice-free during winter. Owing to the pronounced hydrographical

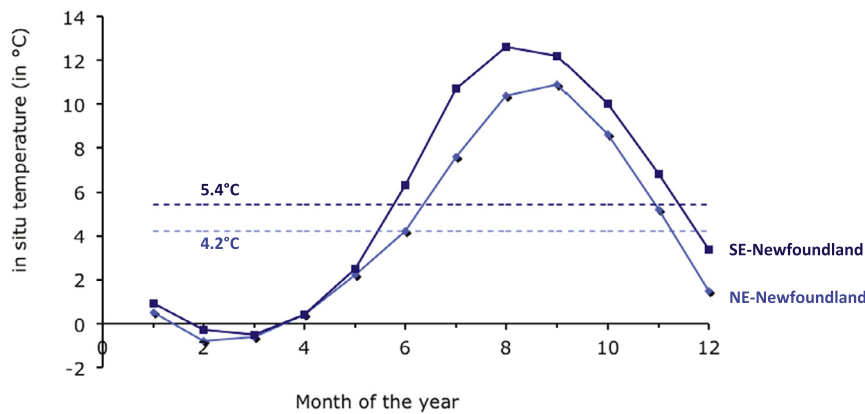


Fig. 5. Monthly mean temperature at the NE Newfoundland site (Bonavista Bay) in light blue, and at SE Newfoundland (Placentia Bay) in dark blue. Data have been obtained from the OES database (http://www2.mar.dfo-mpo.gc.ca/science/ocean/coastal_temperature/coastal_temperature.html) in area 3Lb for the NE Newfoundland site and 3Ps for SE Newfoundland. Dotted lines represent annual means at both sites. (For interpretation of the references to color in this figure legend, the reader is referred to the web version of this article.)

gradients in the Newfoundland region, distinct biological seasonal patterns occur over rather short distances (Nezlin et al., 2002). Off NE Newfoundland, where the influence of the LC is stronger, primary production follows a typical Arctic regime with a slow increase from January to June, followed by a decrease towards stable values from August to December. Off SE Newfoundland, less impacted by the LC, phytoplankton blooms in spring and fall, as generally observed at mid-latitudes. These differences are primarily ascribed to the water column structure affecting light and nutrient conditions in the upper layer (Nezlin et al., 2002). Under strong turbulent mixing conditions such as those in LC waters (NE Newfoundland), nutrients are available, but cells tend to disperse into deeper layers where light becomes limiting for phytoplankton growth. As the water column stabilizes, primary production progressively increases and reaches its highest level relatively late (spring/summer). In contrast, generally weaker mixing in the less turbulent waters off SE Newfoundland allows for a phytoplankton bloom already in early spring, resulting in alkenone production at cooler temperatures than off NE Newfoundland. In addition, along NE Newfoundland sea ice generally persists until early May, while waters offshore SE Newfoundland are usually ice-free all year. An earlier phytoplankton blooming in ice-free waters off SE Newfoundland would result in colder alkenone (early spring) SSTs compared to NE Newfoundland where alkenone production would not take place until sea ice has melted (late spring–summer). A positive temperature offset was previously reported off North Iceland (Sicre et al., 2011), close to the polar front where, during heavy ice years, alkenone-SSTs appear systematically biased towards warmer months when compared to instrumental data, suggesting that sea ice retarded the spring bloom. We can thus conclude that both turbulent conditions and sea ice occurrence likely contribute to a shift towards warmer values of the alkenone-derived SSTs in NE Newfoundland. Higher values by $\sim 1^\circ\text{C}$ off NE Newfoundland ($4.5\text{--}5.5^\circ\text{C}$) as compared to SE Newfoundland ($3.5\text{--}4.5^\circ\text{C}$) would thus reflect delayed blooming (Nezlin et al., 2002) due to the presence of sea ice (Sicre et al., 2011).

Fig. 4 shows the time-series (Fig. 4b, c) at both sites and the NAM index (Fig. 4a). Proxy records NE and SE of Newfoundland exhibit decadal-scale variability superimposed on a general cooling trend and show differences over the common time window (1930–2007). Correlations were calculated between SSTs and NAM index values for the two cores (AI07-04BC and AI07-11BC). The number of degrees of freedom between the two time series was computed following Bretherton et al. (1999), taking into account the autocorrelation of each time series. Because alkenone-derived SSTs represent an average value over the sediment sampling step

(1 cm and 0.5 cm for the top two cms), correlations were calculated between SSTs and the NAM index value averaged over the time interval of each sediment layer, i.e. corresponding to 1 cm in most of the core and 0.5 cm at the top. We found that the NE Newfoundland SSTs are negatively correlated with the NAM index average over the same time interval as the SSTs ($r = -0.63$, with $p < 0.05$ according to a 2-sided Student test and with 23 degrees of freedom). The statistical significance of this correlation is confirmed by a bootstrap approach with 1000 permutations. In particular, lowest SST values are reached during the late 1980s and early 1990s of high ^+NAM (Drinkwater, 1996; Morison et al., 2012), as expected from strong NW winds. Increased sea ice has previously been described for the same period (Weckström et al., 2013). Conversely, correlation between NAM and SSTs off SE Newfoundland is not significantly different from 0 at the 95% confidence level ($r = 0.07$). Local atmospheric and hydrographical conditions most likely explain the different SSTs/NAM relationship. While the NE Newfoundland site is located in the subpolar zone which strongly responds to NAM today (Thompson and Wallace, 1998), the SE Newfoundland site is transitional in-between subpolar and subtropical climate influences and also reflects the (sub)tropical ocean signal propagated by the NAC. Correlations between proxy SSTs and the NAM index at both sites are fully consistent with the modern SST/NAO correlation map for in the North Atlantic region (Marshall et al., 2001) and subsequently reinforce our interpretation of the two proxy records. Even more importantly, the remarkable agreement with Marshall et al. (2001) emphasizes that our SST records are of large-scale significance.

3.2. SST variability over the last two millennia

SSTs of the last ~ 2000 -yr from NE and SE Newfoundland were reconstructed from two gravity cores (AI07-03G; AI07-12G) and compared with SSTs from N. Iceland (Figs. 1 and 6). Due to minor losses of surficial sediments during the coring operation, the core-top ages are estimated to be 1775 AD for AI07-03G and 1770 AD for AI07-12G. Off NE Newfoundland, SSTs range between 4.5 and 6°C and show decadal-scale variability with a colder interval at 1000–1350 AD, approximately concurrent with the Medieval Climate Anomaly (MCA) (Fig. 6b). Both the well-defined onset and termination of this interval occurred within only a few decades. During the Little Ice Age (LIA), SSTs are generally warmer than during the MCA, showing marked warm spells at $\sim 1470\text{--}1480$ AD and cold ones at $\sim 1440\text{--}1460$ AD and $\sim 1710\text{--}1750$ AD. In contrast, SSTs off SE Newfoundland rapidly decrease until ~ 1000 AD and thereafter fluctuate around $\sim 4^\circ\text{C}$ (Fig. 6c). The absence of contrasting MCA/LIA conditions here is notable and consistent with

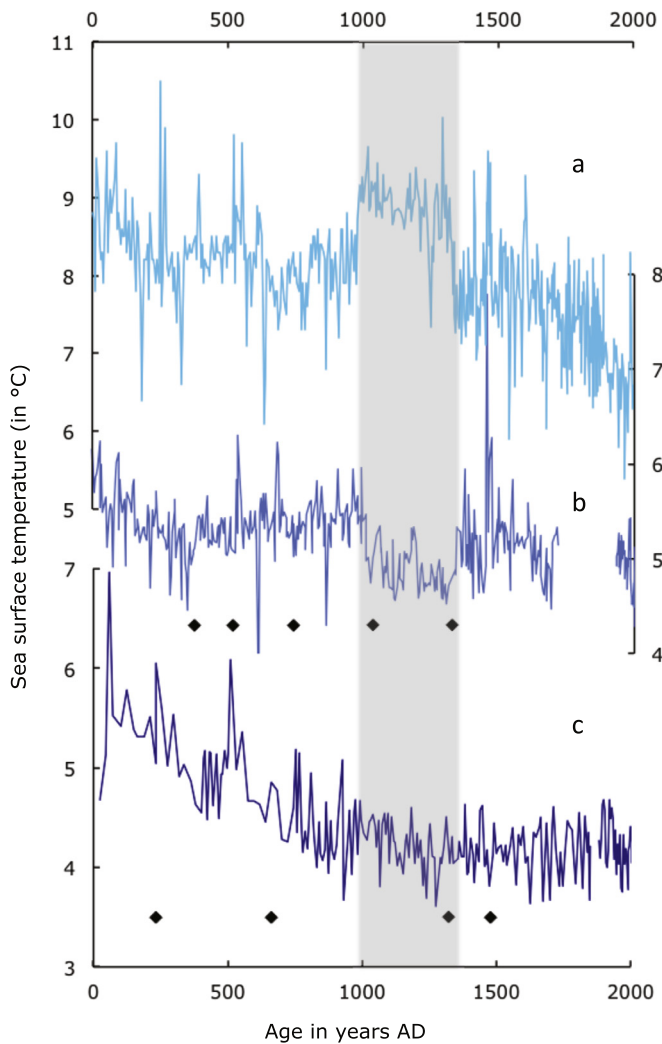


Fig. 6. SST proxy reconstructions for the last 2000 years from off Newfoundland and North Iceland. Alkenone-derived SST reconstruction from (a) Off North Iceland obtained from the Calypso core MD99-2275 (Sicre et al., 2011) (b) NE Newfoundland obtained from gravity core AI07-03G and from box-core AI07-04BC for the upper part, and (c) SE Newfoundland obtained from gravity core AI07-12G and from box-core AI07-11BC for the upper part. The grey shading broadly indicates the Medieval Climate Anomaly (MCA). Black diamonds indicate AMS ^{14}C -dated sediment layers used to build the age model.

dinocyst data from the same core (Solignac et al., 2011) as well as with alkenone data off Nova Scotia (Keigwin et al., 2003). At the NE site, dinocyst variability was even smaller, being primarily affected by freshwater supply and productivity during this time interval (Solignac et al., 2011).

The two sites thus clearly show different oceanographic patterns during the last 2000 years. The SE site mainly illustrates the general late Holocene cooling trend of the North Atlantic region with little or no clear difference between the MCA and LIA. In contrast, the NE Newfoundland site shows strong multi-centennial SST variability and colder SSTs during the MCA. This surface-water cooling can be compared to the present-day ocean response to strong NW winds during ^{+}NAM years (Drinkwater, 1996; Morison et al., 2012) (Fig. 4). Likewise, warmer SSTs before 1000 AD and after 1350 AD (LIA) can be linked to LC weakening as a result of reduced NW winds combined with more frequent southerly winds during ^{-}NAM years (Morison et al., 2012). Note that the MCA cooling in NE Newfoundland corresponds to a warming of a similar magnitude ($\sim 1^{\circ}\text{C}$) observed in North Iceland shelf waters (Figs. 1, 6a; MD99-2275), which has been attributed to ^{+}NAM -type atmospheric circulation and an enhanced AMOC (Sicre et al., 2011;

Trouet et al., 2009). Previous low-resolution SST reports from the NW Atlantic also hypothesized ^{+}NAO -like conditions during the MCA (Keigwin, 1996; Seidenkrantz et al., 2007, 2008). Furthermore, higher proportions of subpolar waters at intermediate depths evidenced at the Rockall Trough (Copard et al., 2012) are in agreement with stronger Westerlies and intensified SPG circulation in a ^{+}NAM scenario. This coherent regional pattern of proxy records is overall consistent with the Trouet et al. (2009) and Olsen et al. (2012) long-term reconstructions of the NAO index and the suggestion of a persistent positive phase during the MCA (Seidenkrantz et al., 2007, 2008; Trouet et al., 2009, 2012; Ribeiro et al., 2012; Andresen et al., 2013). Although this mode of variability operates mainly at interannual time scales, the SST/NAO correlation tripole shows a pronounced signature at decadal time scales as well (Marshall et al., 2001) suggesting the role of NAM on climate at lower frequency (Boessenkool et al., 2007).

Enhanced AMOC and northward heat transport during the MCA could also have triggered coastal glacier melting, subsequently increasing the discharge of cold/melt waters into Greenland coastal waters, while further offshore, the warm Irminger Sea Water signal was still present. This pattern has been documented in several studies showing surface-water cooling and/or increased sea-ice during the MCA in coastal W/SW-Greenland sites (Jensen et al., 2004; Seidenkrantz et al., 2007, 2008; Andresen et al., 2011), while elevated SSTs were observed further offshore between ~ 1000 – 1350 AD (Ribeiro et al., 2012) and 800 – 1330 AD (Sha et al., 2012). Therefore, apart from the SST response to direct wind forcing, colder LC waters during the MCA may also in part reflect advection of freshwater and ice by the WGC (Morison et al., 2012), since south of David Strait the majority of this flow turns westwards and reaches the continental slope of W-Labrador (Fig. 1) (Schmidt and Send, 2007). Moreover, as outlined before (see Fratantoni and McCartney, 2010), a re-routing of Arctic waters through the Canadian Archipelago may be another important factor explaining negative SST anomalies of the LC during Medieval times.

During the LIA, warmer SSTs found along NE Newfoundland coincide with colder and heavy ice years off North Iceland (Massé et al., 2008). This pattern compares well with surface ocean conditions during ^{-}NAM years, the GSA being an extreme example. Large quantities of freshwater and ice exported through Fram Strait (Dickson et al., 1996) contribute to the reduction of Labrador Sea convection. Thus, NAM not only affects local climate through wind forcing but also exerts control on the convective activity of the Labrador region by activating either the *Fram Strait Route* (^{-}NAM) or the *Canadian Archipelago Route* (^{+}NAM), with different consequences for the AMOC.

4. Conclusions

Our two distinct SST records, one within the LC (NE Newfoundland) and the other at the northern edge of the NAC (SE Newfoundland), provide new insight into the overall interaction between the LC and the NAC. The SE Newfoundland SST record reveals an overall weaker influence of the NAC through the last 2000 years with only little variability at (multi)centennial scale. In contrast, the NE Newfoundland record shows that LC circulation is tightly linked to Arctic atmospheric conditions (NAM), which in turn modulate the advection pathway of cold, ice-loaded Polar Waters from the Arctic. This is illustrated by virtue of a generally enhanced LC during the MCA, and an overall weaker LC and likely decreased AMOC during the LIA (Lund et al., 2006). If this MCA/LIA pattern is to be considered analogous to generally warmer/colder climates in the subpolar North Atlantic, it would suggest the possibility of increasing LC strength in a future warmer climate. This would not only imply a colder future climate off eastern Canada,

but would also affect regional ocean–atmosphere interaction off Newfoundland, deep convection in the Labrador Sea, NAC heat transport, and thus, climate in the larger North Atlantic realm.

Acknowledgements

The research presented here was supported by the French LEFE/INSU NAIV project (CNRS/INSU) and the ERC 203441 starting grant ICEPROXY project. K.W. was funded via a Marie Curie IEF grant (agreement No. 236678). M.-S.S. and A.K. received funding via the TROPOLINK and OCEANHEAT projects supported by the Danish Council for Independent Research Natural Science (FNU Grants 09-069833 and 12-126709). The cruise was funded by the Danish Council for Independent Research, Natural Science (project No. 272-06-0604/FNU) and carried out within the Danish–Russian collaboration project ‘Joint paleoceanographic investigations in the Labrador Sea region’. This work is a contribution to the EU FP7 project ‘Past4Future’ (project No. 243908).

References

- Aksenov, Y., Bacon, S., Coward, A.C., Holliday, N.P., 2010. Polar outflow from the Arctic Ocean: a high-resolution model study. *J. Mar. Syst.* 83, 14–37.
- Andresen, C.S., McCarthy, D.J., Dylmer, C.V., Seidenkrantz, M.-S., Kuijpers, A., Lloyd, J.M., 2011. Interaction between subsurface ocean waters and calving of Jakobshavn Isbræ during the late Holocene. *Holocene* 21, 211–224.
- Andresen, C.S., Hansen, M.J., Seidenkrantz, M.-S., Jennings, A.E., Knudsen, M.F., Nørgaard-Pedersen, N., Larsen, N.K., Kuijpers, A., Pearce, C., 2013. Mid- to late-Holocene oceanographic variability on the Southeast Greenland shelf. *Holocene* 23 (2), 167–178. <http://dx.doi.org/10.1177/0959683612460789>.
- Boessenkool, K.P., Hall, I.R., Elderfield, H., Yashayaev, I., 2007. North Atlantic climate and deep-ocean flow speed changes during the last 230 years. *Geophys. Res. Lett.* 34, L13614. <http://dx.doi.org/10.1029/2007GL030285>.
- Bretherton, C.S., Widmann, M., Dymnikov, V.P., Wallace, J.M., Blade, I., 1999. Effective number of degrees of freedom of a spatial field. *J. Climate* 12, 1990–2009.
- Copard, K., Colin, C., Henderson, G.M., Scholten, J., Douville, E., Sicre, M.-A., Frank, N., 2012. Late Holocene intermediate water variability in the Northeastern Atlantic as recorded by deep-sea corals. *Earth Planet. Sci. Lett.* 313–314, 34–44.
- Cunningham, L.K., Austin, W.E.N., Knudsen, K.-L., Eiriksson, J., Scourse, J., Wanamaker Jr., A., Butler, P., Cage, A., Kristensen, D.K., Richter, T., Husum, K., Hald, M., Andersson, C., Zorita, E., Linderholm, H., Gunnarson, B., Sicre, M.-A., Sejrup, H.P., Jiang, H., Wilson, R.J.S., 2013. Reconstructions of surface ocean conditions from the North East Atlantic and Nordic Seas during the last millennium. *Holocene* 23 (7), 921–935.
- Czaja, A., Frankignoul, C., 2002. Observed impact of Atlantic SST anomalies on the North Atlantic Oscillation. *J. Climate* 15, 606–623.
- Dickson, R.R., Meincke, J., Malmgren, S.-A., Lee, J.A., 1988. The great salinity anomaly in the Northern North Atlantic 1968–1982. *Prog. Oceanogr.* 20, 103–151.
- Dickson, R.R., Lazier, J., Meincke, J., Rhines, P., Swift, J., 1996. Long-term coordinated change in the convective activity of the north Atlantic. *Prog. Oceanogr.* 38, 241–295.
- Drinkwater, K.F., 1996. Climate and oceanographic variability in the Northwest Atlantic during the 1980s and early-1990s. *J. Northwest Atl. Fish. Sci.* 18, 77–97.
- Fratantoni, P.S., McCartney, M.S., 2010. Freshwater export from the Labrador Current of the north Atlantic Current at the Tail of the Grand Banks of Newfoundland. *Deep-Sea Res.* 1 57, 258–283.
- Jensen, K.G., Kuijpers, A., Koç, N., Heinemeier, J., 2004. Diatom evidence of hydrographic changes and ice conditions in Igaliku Fjord, South Greenland, during the past 1500 years. *Holocene* 14, 152–164.
- Jessen, C.A., Solignac, S., Nørgaard-Pedersen, N., Mikkelsen, N., Kuijpers, A., Seidenkrantz, M.-S., 2011. Exotic pollen as an indicator of variable atmospheric circulation over the Labrador Sea region during the mid to late Holocene. *J. Quat. Sci.* 26 (3), 286–296. <http://dx.doi.org/10.1002/jqs.1453>.
- Jones, E.P., Anderson, L.G., 2008. Is the global conveyor belt threatened by Arctic Ocean fresh water outflow? In: Dickson, R.R., Meincke, J., Rhines, P. (Eds.), *Arctic-Subarctic Ocean Fluxes*. Springer, Berlin, pp. 385–404.
- Keigwin, L.D., 1996. The little Ice Age and Medieval Warm Period in the Sargasso Sea. *Science* 274, 1504–1508.
- Keigwin, L., Sachs, J.P., Rosenthal, Y., 2003. A 1600-year history of the Labrador Current off Nova Scotia. *Clim. Dyn.* 21, 53–62.
- Lazier, J.R.N., Wright, D.G., 1993. Annual velocity variations in the Labrador Current. *J. Phys. Oceanogr.* 23, 659–678.
- Lund, D.C., Lynch-Stieglitz, J., Curry, W.B., 2006. Gulf Stream density structure and transport during the past millennium. *Nature* 444, 601–604.
- Marshall, J., Kushnir, Y., Battisti, D., Chang, P., Czaja, A., Dickson, R., McCartney, M., Saravanan, R., Visbeck, M., 2001. North Atlantic Climate variability: phenomena, impacts and mechanisms. *Int. J. Climatol.* 21, 1863–1898.
- Massé, G., Rowland, S., Sicre, M.-A., Jacob, J., Jansen, E., Belt, S., 2008. Abrupt climate changes for Iceland during the last millennium. Evidence from high resolution sea ice reconstructions. *Earth Planet. Sci. Lett.* 269, 565–569.
- Morison, J., Kwok, R., Peralta-Feriz, C., Alkire, M., Rigor, I., Andersen, R., Steele, M., 2012. Changing Arctic Ocean freshwater pathways. *Nature* 481, 66–70.
- Nezlin, N.P., Afanasyev, D., Ginzburg, A.I., Kostianoy, A.G., 2002. Remotely sensed studies of phytoplankton dynamics under physical forcing in different ocean regions. *Adv. Space Res.* 29, 99–106.
- Olsen, J., Anderson, J.N., Knudsen, M.F., 2012. Variability of the North Atlantic Oscillation over the past 5,200 years. *Nat. Geosci.* 5, 808–812. <http://dx.doi.org/10.1038/ngeo1589>.
- PAGES 2k Consortium, 2013. Continental-scale temperature variability during the past two millennia. *Nat. Geosci.* 6, 339–346. <http://dx.doi.org/10.1038/ngeo1797>.
- Prahl, F.G., Muehlhausen, L.A., Zahnle, D.L., 1988. Further evaluation of long-chain alkenones as indicators of paleoceanographic conditions. *Geochim. Cosmochim. Acta* 52, 2303–2310.
- Reimer, P.J., Baillie, M.G.L., Bard, E., Bayliss, A., Beck, J.W., Blackwell, P.G., Ramsey, C.B., Buck, C.E., Burr, G.S., Edwards, R.L., Friedrich, M., Grootes, P.M., Guilderson, T.P., Hajdas, I., Heaton, T.J., Hogg, A.G., Hughen, K.A., Kaiser, K.F., Kromer, B., McCormac, F.G., Manning, S.W., Reimer, R.W., Richards, D.A., Southon, J.R., Talamo, S., Turney, C.S.M., van der Plicht, J., Weyhenmeyer, C.E., 2009. IntCal09 and Marine09 Radiocarbon Age calibration curves, 0–50,000 years cal BP. *Radiocarbon* 51 (4), 1111–1150.
- Ribeiro, S., Moros, M., Ellegaard, M., Kuijpers, A., 2012. Climate variability in West Greenland through the past 1500 years: evidence from a high-resolution marine palynological record from Disko Bay. *Boreas* 41, 68–83.
- Schmidt, S., Send, U., 2007. Origin and composition of seasonal Labrador Sea freshwater. *J. Phys. Oceanogr.* 37, 1145–1154.
- Schmidt, S., Howa, H., Mouret, A., Lombard, F., Anschutz, P., Labeyrie, L., 2009. Particle fluxes and recent sediment accumulation on the Aquitanian margin of Bay of Biscay. *Cont. Shelf Res.* 29, 1044–1052.
- Seidenkrantz, M.-S., Aagaard-Sørensen, S., Møller, H.S., Kuijpers, A., Jensen, K.G., Kundendorf, H., 2007. Hydrography and climatic change during the last 4,400 years in Ameralik Fjord, SW Greenland. *Holocene* 17, 387–401.
- Seidenkrantz, M.-S., Roncaglia, L., Fischer, A., Heilmann-Clausen, C., Kuijpers, A., Moros, M., 2008. Variable North Atlantic climate seesaw patterns documented by a late Holocene marine record from Disko Bugt, West Greenland. *Mar. Micropaleontol.* 68, 66–83.
- Sha, L., Jang, H., Knudsen, K.-L., 2012. Diatom evidence of climatic change in Holsteinborg Dyb, West of Greenland, during the last 1200 yrs. *Holocene* 22, 347–358.
- Sicre, M.-A., Hall, I.R., Mignot, J., Khodri, M., Ezat, U., Truong, M.-X., Eiriksson, J., Knudsen, K.-L., 2011. Sea surface temperature variability in the subpolar Atlantic over the last two millennia. *Paleoceanography* 26, PA4218.
- Solignac, S., Seidenkrantz, M.-L., Jessen, C., Kuijpers, A., Gunvald, A.K., Olsen, J., 2011. Late-Holocene sea-surface conditions offshore Newfoundland based on dinoflagellate cysts. *Holocene* 2, 1–14.
- Ternois, Y., Sicre, M.-A., Boireau, A., Marty, J.-C., Miquel, J.-C., 1996. Production pattern of alkenones in the Mediterranean Sea. *Geophys. Res. Lett.* 23, 3171–3174.
- Thompson, D.W.J., Wallace, J.M., 1998. The Arctic Oscillation signature in the wintertime geopotential height and temperature fields. *Geophys. Res. Lett.* 25, 1297–1300.
- Trouet, V., Esper, J., Graham, N.E., Baker, A., Scourse, J.D., Frank, D.C., 2009. Persistent positive North Atlantic Oscillation mode dominated the Medieval Climate Anomaly. *Science* 324, 78–80.
- Trouet, V., Scourse, J.D., Raible, C.C., 2012. North Atlantic storminess and Atlantic Meridional overturning circulation during the last millennium: reconciling contradictory proxy records of NAO variability. *Glob. Planet. Change* 84–85, 48–55. <http://dx.doi.org/10.1016/j.gloplacha.2011.10.003>.
- Weckström, K., Massé, G., Collins, L.G., Hanhijärvi, S., Bouloubassi, I., Sicre, M.-A., Seidenkrantz, M.-S., Schmidt, S., Andersen, T.J., Andersen, M.L., Hill, B., Kuijpers, A., 2013. Evaluation of the sea ice proxy IP25 against observational and diatom proxy data in the SW Labrador Sea. *Quat. Sci. Rev.* 79, 53–62. <http://dx.doi.org/10.1016/j.quascirev.2013.02.012>.